Molecular and Cellular Endocrinology 412 (2015) 148–158

Contents lists available at ScienceDirect

Molecular and Cellular Endocrinology

journal homepage: www.elsevier.com/locate/mce

Inhibition of platelet-derived growth factor (PDGF) receptor affects follicular development and ovarian proliferation, apoptosis and angiogenesis in prepubertal eCG-treated rats

Natalia Pascuali [a], Leopoldina Scotti [a], Dalhia Abramovich [a], Griselda Irusta [a], Mariana Di Pietro [a], Diana Bas [a], Marta Tesone [a,b], Fernanda Parborell [a,*]

[a] Instituto de Biología y Medicina Experimental (IByME), CONICET, Buenos Aires, Argentina
[b] Departamento de Química Biológica, Facultad de Ciencias Exactas, Universidad de Buenos Aires, Buenos Aires, Argentina

ARTICLE INFO

Article history:
Received 14 January 2015
Received in revised form 24 April 2015
Accepted 24 April 2015
Available online 29 April 2015

Keywords:
Ovary
Platelet-derived growth factor
Folliculogenesis
Apoptosis
Angiogenesis

ABSTRACT

The platelet-derived growth factor (PDGF) system is crucial for blood vessel stability. In the present study, we evaluated whether PDGFs play a critical intraovarian survival role in gonadotropin-dependent folliculogenesis. We examined the effect of intrabursal administration of a selective platelet-derived growth factor receptor (PDGFR) inhibitor (AG1295) on follicular development, proliferation, apoptosis and blood vessel formation and stability in ovaries from rats treated with equine chorionic gonadotropin (eCG). The percentages of preantral follicles (PAFs) and early antral follicles (EAFs) were lower in AG1295-treated ovaries than in control ovaries ($p < 0.01$–0.05). The percentage of atretic follicles (AtrFs) increased in AG1295-treated ovaries compared to control ($p < 0.05$). The ovarian weight and estradiol concentrations were lower in AG1295-treated ovaries than in the control group ($p < 0.01$ and $p < 0.05$, respectively), whereas progesterone concentrations did not change. AG1295 decreased the proliferation index in EAFs ($p < 0.05$) and increased the percentage of nuclei positive for cleaved caspase-3 and apoptotic DNA fragmentation ($p < 0.01$–0.05). AG1295 increased the expression of Bax ($p < 0.05$) without changes in the expression of Bcl-2 protein. AG1295-treated ovaries increased the cleavage of caspase-8 ($p < 0.05$) and decreased AKT and BAD phosphorylation compared with control ovaries ($p < 0.05$). AG1295 caused a decrease not only in the endothelial cell area but also in the area of pericytes and vascular smooth muscle cells (VSMCs) in the ovary ($p < 0.05$). Our findings suggest that the local inhibition of PDGFs causes an increase in ovarian apoptosis through an imbalance in the ratio of antiapoptotic to proapoptotic proteins, thus leading a larger number of follicles to atresia. PDGFs could exert their mechanism of action through an autocrine/paracrine effect on granulosa and theca cells mediated by PDGFRs. In conclusion, these data clearly indicate that the PDGF system is necessary for follicular development induced by gonadotropins.

© 2015 Elsevier Ireland Ltd. All rights reserved.

1. Introduction

The development of new blood vessels in the ovary is essential to guarantee the necessary supply of nutrients and hormones to promote follicular growth and corpus luteum formation (Redmer and Reynolds, 1996; Suzuki et al., 1998). While vascular endothelial growth factor (VEGF) is the main initiator of angiogenesis, the coordinated action of various factors is necessary for the formation and differentiation of mature vascular networks (Fraser and Wulff, 2003; Kaczmarek et al., 2005). These factors include angiopoietins (ANGPTs), transforming growth factor beta (TGF-β) and platelet-derived growth factors (PDGFs) (Robinson et al., 2009). PDGFs are members of a family of homo- or heterodimers assembled by four different polypeptide chains encoded by four different genes, which comprise the classical A and B chains (Claesson-Welsh, 1996; Heldin and Westermark, 1999) in addition to the more recently discovered C and D chains (LaRochelle et al., 2001; Li et al., 2000). These chains can form five dimeric isoforms: PDGF-AA, PDGF-AB, PDGF-BB, PDGF-CC and PDGF-DD, which exert their effects through binding and activation of tyrosine kinase receptors, PDGF receptor alpha (PDGFRα) and PDGF receptor beta (PDGFRβ) (Heldin and Westermark, 1999). PDGFs are widely expressed in different adult cell types, including platelets, smooth muscle cells and endothelial cells (Heldin and Westermark, 1999; Hwu et al., 2009). Upon activation, their receptors PDGFRα and β trigger responses involved both in physiological and pathological

* Corresponding author. Instituto de Biología y Medicina Experimental, Vuelta de Obligado 2490, C1428ADN Buenos Aires, Argentina. Tel.: +1147832869; fax: +54 011 4786 2564.
E-mail address: fparborell@gmail.com (F. Parborell).

http://dx.doi.org/10.1016/j.mce.2015.04.021
0303-7207/© 2015 Elsevier Ireland Ltd. All rights reserved.

processes, which include cell growth and survival (Huang et al., 1984; Rocha et al., 2007), cell migration (Yu et al., 2001), vascular permeability (Uren et al., 1994), and wound healing (Heldin et al., 1998). Besides, PDGFs are potent angiogenic factors, which recruit smooth muscle cells and pericytes to stabilize blood vessels (Heldin and Westermark, 1999; Hellstrom et al., 1999).

The expression of all members of the PDGF family has been previously described in the rat, mouse, porcine and human ovary (May et al., 1992; Pinkas et al., 2008; Sleer and Taylor, 2007a; Yoon et al., 2006). In rat, protein expression of PDGF ligands and receptors has been identified in oocytes of primordial, primary and developing follicles, while only PDGF-A and PDGFR-α have been found in granulosa from secondary stages onwards (Nilsson et al., 2006; Sleer and Taylor, 2007a). A study in mice has shown that oocytes, granulosa and theca cells of growing follicles express all isoforms of PDGF and PDGFR-β, whereas PDGFR-α is highly expressed in primordial, primary and secondary follicles (Yoon et al., 2006). Pinkas et al. (2008) reported PDGF-A and -B protein expression in oocytes and granulosa cells of human follicles and PDGFR-β, but not PDGFR-α, in granulosa cells from primary follicles (Pinkas et al., 2008). In addition, these authors suggested that binding of PDGF ligands to their receptors may act as a signaling factor promoting the activation of primordial follicles (Nilsson et al., 2006; Pinkas et al., 2008; Sleer and Taylor, 2007a; Yoon et al., 2006). Furthermore, PDGFs stimulate in vitro proliferation of theca cells from antral follicles from rats (Duleba et al., 1999) and pigs (May et al., 1992). Nonetheless, the precise role of PDGFs in ovarian folliculogenesis is yet unknown.

In this study, we hypothesized that apoptotic cell death in granulosa and theca cells of antral follicles selected for ovulation can be prevented by paracrine and/or autocrine actions of PDGFs. Son et al. (2014) have recently demonstrated that PDGF-C induces anti-apoptotic effects on human macrophages through AKT activation and proapoptotic BAD phosphorylation, which results in BAD inactivation (Son et al., 2014). In cultured rat pericytes, PDGF-B induces cell growth and antiapoptotic responses through AKT (Arimura et al., 2012). It is known that FSH and LH are the prime survival factors for ovarian follicles and that their antiapoptotic effects are probably mediated by the production of ovarian growth factors. Several authors and our group have demonstrated that various growth factors (such as insulin-like growth factor 1, epidermal growth factor, transforming growth factor-α and fibroblast growth factors 2 and 7) prevent apoptosis in rat follicles (Chun et al., 1994; McGee et al., 1999; Parborell et al., 2001; Tilly et al., 1992, 1995). Besides, we have previously shown that inhibition of VEGF and ANGPT1 activity in rats increases the number of atretic follicles mediated by ovarian apoptosis through an imbalance in the ratio of antiapoptotic to proapoptotic proteins, suggesting that both angiogenic factors are required for the follicular development induced by gonadotropins (Abramovich et al., 2006; Parborell et al., 2008). So far, few studies have evaluated the effect of PDGF inhibition on the ovary. Kuhnert et al. (2008) demonstrated that inhibition of PDGFRβ signaling produces a blockage of pericyte recruitment in the mouse corpus luteum, with the presence of multiple hemorrhages (Kuhnert et al., 2008). Moreover, Sleer and Taylor (2007b) showed that inhibition of PDGFR signaling causes a decrease in the number of corpora lutea per treated ovary in comparison to the contralateral control ovary in gonadotropin-stimulated immature rats (Sleer and Taylor, 2007b). However, the understanding of the distinct roles of PDGFs in follicular and vascular development in the ovary is still limited. To date, no reports have addressed the actions of a PDGF inhibitor on gonadotropin-stimulated follicular development and atresia in the ovary. Therefore, in this study, we specifically investigated whether PDGFs play a critical intraovarian survival role in gonadotropin-dependent folliculogenesis. In particular, we examined the effect of local administration of a PDGFR selective inhibitor on follicular development, proliferation, apoptosis and blood vessel formation and stability in ovaries from prepubertal equine chorionic gonadotropin (eCG)-treated rats.

2. Materials and methods

2.1. Hormones and drugs

PDGFR (platelet-derived growth factor receptor) kinase inhibitor AG1295 (658550) was purchased from Calbiochem (Merck, Darmstadt, Germany). Equine chorionic gonadotropin (eCG) was provided by Syntex S.A. (Buenos Aires, Argentina). Dimethyl sulfoxide (DMSO), NaCl, proteinase K, sodium dodecyl sulfate (SDS), RNase, boric acid, ethylene diamine tetraacetic acid (EDTA), bovine serum albumin (BSA), diethyl ether, methanol, n-hexane, dichloromethane, Na2HPO4, NaH2PO4, sodium azide, gelatin, NP-40, glycerol and Tween-20 were from Sigma-Aldrich (St. Louis, MO, USA), and 3,3′-diaminobenzidine (DAB) was from Roche Applied Science (Mannheim, Germany). The details, suppliers and dilution of antibodies used in this study are reported in Table 1. All other chemicals were of reagent grade and were obtained from standard commercial sources.

2.2. In vivo AG1295 treatment and superovulation

Immature female Sprague–Dawley rats (21–23 days) from our colony were used. Rats were housed at our Institution (Instituto de Biología y Medicina Experimental (IByME), Buenos Aires, Argentina), under 12-hour light/dark cycles and with free access to food and water. Rats were anesthetized with ketamine HCl (80 mg/kg; Holliday-Scott, Buenos Aires, Argentina) and xylazine (4 mg/kg; König Laboratories, Buenos Aires, Argentina). The ovaries were exteriorized through an incision made in the dorsal lumbar region. Subsequently, a selective inhibitor of PDGFR (AG1295, Calbiochem) dissolved in 0.1% DMSO was injected under the bursa of one ovary, in a dose of either 20 or 50 μg/ovary. AG1295 is a low-molecular-weight tyrphostin that specifically inhibits PDGF receptor kinase, blocking PDGF-receptor signal transduction (Banai et al., 1998; Zhang et al., 2012). Moreover, this kind of molecule does not cause the side effects observed with other inhibitors. Unlike larger receptor antibodies, the small size of tyrphostins permits easier access to receptor sites within tissues (Banai et al., 1998; Levitzki and Gazit, 1995). The contralateral ovary was used as a control, receiving DMSO only. An additional control was designed in which one ovary was injected with DMSO (0.1%) and the contralateral ovary was untreated. No significant differences were found in the number of follicles at any stage between the DMSO-injected ovary and the untreated ovary. Therefore, DMSO was chosen as the control. After injection, ovaries were replaced and the incision closed with skin adhesive. Rats were then subcutaneously injected with 0.1 ml eCG (25 IU/rat) to induce follicular development. This experimental design represents a good model to study the effect of different factors on gonadotropin-dependent follicle development since it allows synchronization of the cycles and exogenous control of gonadotropin levels to avoid individual variations (Abramovich et al., 2006; Choi et al., 2010; Dhanasekaran and Moudgal, 1989; Hughes and Gorospe, 1991; Parborell et al., 2008). All animals were euthanized 24 or 48 h after surgery by CO_2 asphyxiation. At least five animals were used for each of the four experimental groups (according to the AG1295 dose and treatment time). The ovaries were removed, weighed and cleaned of adhering tissue in culture medium for subsequent assays. The ovarian weight of the rats is expressed as the weight of individual ovaries.

All experiments were approved in advance by the Animal Experimentation Committee of the IByME and were conducted in accordance with the guidelines provided by the Office of Animal Care and Use (National Institutes of Health, USA).

Table 1
Antibodies used in immunohistochemistry (IHC) and Western blot.

Antibody target	Host/Type	Catalog No.	Supplier	Technique	Dilution
Primary antibodies					
PCNA	Rabbit polyclonal	sc-7907	Santa Cruz Biotechnology, Inc.[a]	IHC	1:100
Caspase-3 (cleaved)	Rabbit polyclonal	CP229	Biocare Medical[b]	IHC	1:100
von Willebrand factor	Rabbit polyclonal	A0082	Dako[c]	IHC	1:200
α-Smooth muscle actin	Mouse monoclonal	ab18147	Abcam[d]	IHC	1:200
Bax	Rabbit polyclonal	sc-493	Santa Cruz Biotechnology, Inc.[a]	Western blot	1:300
Bcl-2	Rabbit polyclonal	sc-492	Santa Cruz Biotechnology, Inc.[a]	Western blot	1:200
Bcl-$X_{L/S}$	Rabbit polyclonal	sc-634	Santa Cruz Biotechnology, Inc.[a]	Western blot	1:100
FAS	Rabbit polyclonal	sc-7886	Santa Cruz Biotechnology, Inc.[a]	Western blot	1:200
FASL	Rabbit polyclonal	sc-956	Santa Cruz Biotechnology, Inc.[a]	Western blot	1:200
Caspase-8 (cleaved)	Rabbit polyclonal	sc-7890	Santa Cruz Biotechnology, Inc.[a]	Western blot	1:200
AKT	Rabbit polyclonal	#9272	Cell Signaling Technology[e]	Western blot	1:200
Phospho-Akt (Ser473)	Rabbit polyclonal	#9271S	Cell Signaling Technology[e]	Western blot	1:200
BAD	Rabbit polyclonal	#9292	Cell Signaling Technology[e]	Western blot	1:200
Phospho-BAD (ser136)	Rabbit polyclonal	#9295S	Cell Signaling Technology[e]	Western blot	1:400
β-Actin	Rabbit polyclonal	sc-1616	Santa Cruz Biotechnology, Inc.[a]	Western blot	1:3000
Secondary antibodies					
Rabbit IgG (biotinylated)	Goat polyclonal	BA-1000	Vector Laboratories[f]	IHC	1:400
Mouse IgG (biotinylated)	Goat polyclonal	BA-9200	Vector Laboratories[f]	IHC	1:400
Rabbit IgG (conjugated to HRP)	Goat polyclonal	A4914	Sigma-Aldrich[g]	Western blot	1:1000

[a] Santa Cruz Biotechnology, Inc., Santa Cruz, CA, USA.
[b] Biocare Medical (Concord, CA, USA).
[c] Dako (Glostrup, Denmark).
[d] Abcam (Cambridge, Massachusetts, USA).
[e] Cell Signaling Technology (Beverly, MA, USA).
[f] Vector Laboratories, (Burlingame, CA, USA).
[g] Sigma-Aldrich (St. Louis, MO, USA).
IHC, immunohistochemistry; Ig, immunoglobulin; HRP, horse radish peroxidase.

2.3. Ovarian morphology

After removal, the ovaries were immediately fixed in 4% paraformaldehyde for 12 h, dehydrated in a graded series of ethanol and embedded in paraffin. To prevent counting the same follicle twice, 5-μm step sections were mounted at 50-μm intervals onto microscope slides according to the method described by Woodruff et al. (1988). To count the number of different stages of follicles per ovary section, slides were stained with hematoxylin and eosin (H&E). Follicles were classified into the following groups: preantral follicles (PAFs), early antral follicles (EAFs), mature antral follicles (MAFs), preovulatory follicles (POFs) and atretic follicles (AtrFs). PAFs have two to four layers of granulosa cells, whereas in EAFs there are more than five layers of granulosa, follicular fluid begins to accumulate and the antral cavity develops (McNatty et al., 1999; Young and McNeilly, 2010). MAFs were defined as follicles that possessed many layers of granulosa and theca cells in mitosis, concomitant with an increase in antrum volume; and POFs were defined as the largest follicles, with the cumulus-oocyte complex protruding into the antrum and located near to the surface of the ovary. AtrFs were defined as those characterized by degeneration and detachment of the granulosa cell layer from the basement membrane, the presence of pyknotic nuclei and oocyte degeneration (Andreu et al., 1998; Sadrkhanloo et al., 1987). The number of PAFs, EAFs, MAFs, POFs and AtrFs was determined in three ovarian sections from each ovary (one control ovary and one treated ovary/animal, five animals per treatment group). The total number of ovarian structures was defined as 100%. Data are expressed as the percentage of each follicle type per ovary.

2.4. Follicle DNA extraction and fragmentation analysis

Individual ovarian follicles were dissected from the ovary under a stereoscopic microscope as previously described (Parborell et al., 2005; Tilly et al., 1992). Briefly, healthy early antral follicles (300–350 μm in diameter) from six ovaries per group were isolated, and the results obtained from each pool were considered a single datum. Cellular DNA was extracted from 10 healthy antral follicles per ovary. Follicles were incubated for 24 h under serum-free conditions at 37 °C in 500 μl of Dulbecco's modified Eagle medium (DMEM) (Gibco®, Thermo Fisher Scientific Inc., Waltham, MA, USA) F12 (1:1) containing 10 mM HEPES, supplemented with fungizone (250 μg/ml), and gentamicin (10 mg/ml) and gassed with 95% O2:5% CO2 at the start of culture. The incubation in serum-free conditions for 24 h allows exhibition of the typical apoptotic DNA ladder. The follicles from each culture were homogenized in a buffer containing 100 mM NaCl, 4 mM EDTA, 50 mM Tris–HCl, 0.5% SDS, pH 8, and proteinase K (100 μg/ml) at 55 °C for 4 h to facilitate membrane and protein disruption. After incubation, samples were cooled on ice in 1 M potassium acetate and 50% chloroform to initiate protein precipitation and then centrifuged at 9000 *g* for 8 min at 4 °C. Supernatants were then precipitated for 30 min in 2.5 volumes of ethanol at –70 °C and centrifuged for 20 min at 5000 *g* at 4 °C. Finally, DNA was extracted in 70% ethanol and resuspended in water. DNA content was measured by reading the absorbance at 260 nm and then incubated for 1 h with RNase (10 μg/ml) at 37 °C. DNA samples were electrophoretically separated on 1.9% agarose gels in TBE buffer (0.089 M Tris:HCl, 0.089 M boric acid, 2 mM EDTA, pH 8). Equal amounts of DNA were loaded into each well (4 μg), together with 3 μl SYBR Green (Thermo Fisher Scientific Inc.). Gel images were captured by the gel documentation system G:BOX iChemi XR (Syngene, UK). Densitometric analysis of low molecular weight (LMW) DNA (<15 kb) was performed using the software program Scion Image for Windows (Scion Corp., Worman's Mill Court, Maryland, USA). Quantitative results obtained by densitometric analysis of the LMW DNA fragments represent the mean ± SEM of three independent gel runs.

2.5. Immunohistochemistry (IHC)

For immunohistochemical localization of proteins, the avidin–biotin–peroxidase complex was used. Five-micrometer sections were mounted at 50-μm intervals onto positively charged slides. Tissue sections were deparaffinized in xylene and rehydrated by

graduated ethanol washes. Endogenous peroxidase activity was blocked with 3% hydrogen peroxide solution and subsequently washed with phosphate buffered saline (PBS) (0.58 M NaCl, 41.56 mM Na2HPO4 anhydrous, 15.8 mM KH2PO4, pH 7.5). Following 10-min citrate antigen retrieval by microwaves (0.01 M citrate buffer, pH 6, 600 W), nonspecific binding was blocked with 2% BSA for 30 min at room temperature (RT).

Sections were incubated with the adequate primary antibody dilution in PBS (PCNA 1:100, cleaved caspase-3 1:100, Von Willebrand factor (VWf) 1:100, α-SMA 1:100) overnight at 4 °C. After washing, slides were incubated with biotinylated anti-rabbit or anti-mouse mouse IgG (1:400) for 30 min at RT. Sections were washed again and incubated for 30 min with avidin-biotinylated horseradish peroxidase complex (Vectastain ABC system; Vector Laboratories, Burlingame, CA, USA). Protein expression was visualized with DAB staining (0.5 mg/ml, 3 min). The reaction was stopped with distilled water and slides were counterstained with hematoxylin and dehydrated before mounting with mounting medium (Canada Balsam Synthetic; Biopack, Buenos Aires, Argentina). Stained sections were analyzed by conventional light microscopy (Nikon, Melville, NY, USA) and digitally photographed at 100× and 400× magnification.

2.6. Evaluation of cell proliferation and apoptosis

Early antral follicles (EAFs) were used for the determination of cell proliferation and apoptosis. Six randomly selected EAFs were photographed from each ovarian section (three sections per ovary; n = 6 animals). These microphotographs were analyzed using the Image J software (Image Processing and Analysis in Java, National Institutes of Health, Bethesda, MD, USA). Percentages of proliferating and apoptotic cells were obtained from PCNA and cleaved caspase-3 immunostaining, respectively. Both parameters were calculated using the Cell Counter tool and the number of immunopositive nuclei was manually determined for each EAF and divided by the total number of nuclei. Images were analyzed separately for the granulosa and theca cell compartments in each EAF at 400×. It is worth mentioning that EAFs were selected since in this stage follicles become most susceptible to atresia. EAFs are considered the most finely regulated checkpoint in folliculogenesis (Chun et al., 1996).

2.7. Evaluation of vascular areas

Microphotographs (six fields/section; three sections/ovary; n = 6 animals) from VWf and α-SMA immunolocalization were also processed using the Image J software (see Supplementary Materials and Methods for further details). The angiogenic parameters measured in sections immunolabeled for VWf (endothelial cell marker) were: relative vascular area (RVA), microvascular density (MVD) and mean cross-sectional area of vessels. Images were analyzed on both stromal and follicular areas.

To quantify RVA, the area occupied by vessels was manually limited, considering as such all immunopositive cells, isolated or in groups, with or without lumen. No immunostained vessel was excluded from the analysis. The total area of the image was measured and the RVA was calculated dividing the absolute vascular area (sum of all vessel areas) by the total image area. MVD was calculated as the total number of vessels in cross-section (CS) per area unit. To quantify the mean cross-sectional area, vessel perimeter was manually outlined in each vessel in CS present in the microphotograph. The area values and number of those cross-sectional vessels were recorded. Finally, the mean cross-sectional area of vessels was calculated as the arithmetic mean of all the vessel area values measured in each image.

The presence of pericytes and VSMCs was detected by immunolabeling with a specific cell marker, α-SMA (Redmer et al., 2001; Robinson et al., 2009). The relative area occupied by mature vessels, the density of mature microvessels and the mean cross-sectional area of mature vessels were calculated as described for VWf.

2.8. Steroid extraction from ovarian tissue

Whole ovaries were mechanically homogenized in acetone (1:10 weight/volume) with an Ultra-Turrax homogenizer (IKA Werk, Breisgau, Germany). Labeled steroids were added as internal standards, with a recovery percentage between 60 and 80%. After 10-min centrifugation (1600 × *g*), supernatants were collected and transferred to conical tubes and evaporated to dryness. Next, 1 ml of distilled water was added to each tube and samples were extracted twice with diethyl ether (1: 2.5 vol/vol). Each time, ether fractions were separated by freezing the samples at –70 °C for 20 min and then transferring the liquid phases to new tubes and evaporating to dryness. The remaining residue was dissolved in 1.4 ml of methanol. After adding 1.4 ml of distilled water to each tube, the samples were subjected to solvent partition with n-hexane. The upper layer was discarded and 2 ml of dichloromethane was added to the lower phase. After mixing for 2 min, the aqueous upper phase was discarded while the lower phase was evaporated to dryness. Finally, residues were resuspended in RIA buffer (Na_2HPO_4 40 mM; NaH_2PO_4 39.5 mM, NaCl 155 mM, sodium azide 0.1%, gelatin 1%, pH = 7.0) and stored at –20 °C until further analysis.

2.9. Radioimmunoassay (RIA)

Steroid concentrations were measured by RIA in control and AG1295-treated ovaries (n = 6/group) (Irusta et al., 2003, 2007). Progesterone (P_4) and estradiol (E_2) concentrations were measured by using specific antibodies supplied by Dr. G.D. Niswender (Animal Reproduction and Biotechnology Laboratory, Colorado State University, Fort Collins, CO, USA). Under these conditions, the intra-assay and interassay variations were 7.2% and 12.5% for E_2 and 8.0 and 14.2% for P_4. The values are expressed as ng hormone/g ovary.

2.10. Western blot analyses

Whole ovaries from six rats were homogenized in five volumes of lysis buffer (20 mM Tris–HCl [pH 8], 137 mM NaCl, 1% NP-40, and 10% glycerol) supplemented with protease inhibitors (0.5 mM PMSF, 0.025 mM *N*-CBZ-L-phenylalanine chloromethyl ketone, 0.025 mM *N*-p-tosyl-lysine chloromethyl ketone, and 0.025 mM L-1-tosylamide-2-phenyl-ethylchloromethyl ketone) (Sigma-Aldrich) and homogenized with an Ultra-Turrax homogenizer. Samples were centrifuged at 4 °C for 10 min at 10,000 × *g*, and the resulting pellets were discarded. Protein concentration in the supernatant was measured by the Bradford assay. After boiling for 5 min, 40 μg of protein was applied to a 12% SDS–polyacrylamide gel, and electrophoresis was performed at 25 mA for 1.5 h. The resolved proteins were transferred for 2 h onto nitrocellulose membranes. The blots were preincubated in blocking buffer (5% nonfat milk and 0.05% Tween-20 in 20 mM triethanolamine-buffered saline [TBS; pH 8.0]) for 1 h at RT and incubated with appropriate primary antibodies in 0.1% Tween–TBS solution overnight at 4 °C. Then, blots were incubated with anti-rabbit or anti-mouse secondary antibodies conjugated with horseradish peroxidase and finally detected by chemiluminescence (ECL; Santa Cruz Biotechnology, Inc., Santa Cruz, CA, USA) and autoradiography with x-ray film (Amersham Hyperfilm ECL®, GE Healthcare, Chalfont, Buckinghamshire, UK). Negative controls were obtained in the absence of the primary antibody. In each experiment, equal amounts of protein were loaded for all samples, and

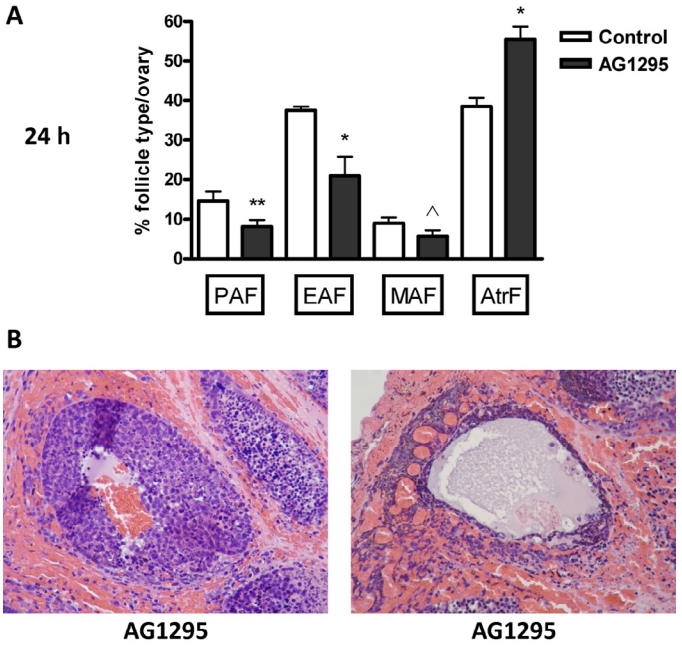

Fig. 1. Effect of AG1295 on folliculogenesis in gonadotropin-stimulated rats. A: Quantification of follicular structures from control and AG1295- treated ovaries (24 h; 20 μg/ovary, n = 5). % PAFs, preantral follicles; % EAFs, early antral follicles; % MAFs, mature antral follicles; % AtrFs, atretic follicles. Data are expressed as mean ± SEM. ^p < 0.1; *p < 0.05; **p < 0.01; paired Student t-test. B: H&E stained sections showing focal regions of hemorrhage only present in AG1295-treated rat ovaries. Note the mass extravasation of erythrocytes into surrounding regions throughout the entire ovary. Arrowheads indicate penetration of erythrocytes into the antral cavity.

both groups were loaded on the same gel. All the gels were run under the same experimental conditions. Protein expression was compared and analyzed with densitometric studies by Scion Image for Windows. The density of each band was normalized to the density of the β-actin band that was used as an internal control. Arbitrary optical density data are expressed as arbitrary units ± SEM.

2.11. Data presentation

The data in the figures and tables are presented as mean ± SEM. Quantitative results obtained by densitometric analysis of the LMW DNA fragments represent the mean ± SEM of three independent gel runs. To quantify protein expression, three independent measurements were performed within each group. Representative gels are shown in the figures. Statistical analysis was performed using paired Student's t-test. Two-tailed values of $p < 0.05$ were considered significant. Statistical analyses were performed with the Prism GraphPad 5.0 software (GraphPad Software, Inc., San Diego, CA, USA).

3. Results

3.1. Ovarian morphology

The effects of PDGFR inhibition on follicle growth are depicted in Fig. 1. Rats were treated with intrabursal injections of either 20 or 50 μg of a selective PDGFR kinase inhibitor, AG1295.

Twenty four hours after AG1295 treatment (20 μg/ovary), the percentage of PAFs and EAFs was lower ($p < 0.01$–0.05) and the percentage of MAFs tended ($p = 0.08$) to be lower than in controls, as shown in Fig. 1A. The percentage of AtrFs was higher in AG1295-treated ovaries than in control ovaries (Fig. 1A; $p < 0.05$). Forty eight hours after AG1295 treatment, the percentage of EAFs tended to be lower ($p = 0.09$) than in controls, whereas there was an increase in the percentage of AtrFs in treated ovaries ($p < 0.05$) (Supplementary Fig. S2). The percentage of POFs was not affected by AG1295 treatment at 24 h (control: 0.18% ± 0.39; AG1295: 0.10 ± 0.28) or 48 h (control: 1.03% ± 1.34; AG1295: 1.71 ± 2.74).

The results obtained with a dose of 50 μg AG1295/ovary were similar to those obtained with a dose of 20 μg/ovary. The percentages of PAFs, EAFs and MAFs decreased significantly after AG1295 treatment while the percentage of AtrFs increased significantly compared to control ovaries (50 μg/ovary, 24 h). Based on these results, the 20 μg/ovary dose and 24-h treatment were used for the following assays.

Ovaries treated with AG1295 showed a great number of hemorrhagic follicles (with the presence of erythrocytes in their antra), together with focal regions of hemorrhage in the stromal tissue (Fig. 1B). Either very few or no hemorrhagic follicles were found in vehicle-injected control ovaries at 24 h (control: 0.15% ± 0.08; AG1295: 6.11 ± 2.54, $p < 0.05$).

Table 2
Effects of AG1295 treatment on ovarian weight and hormone concentrations in gonadotropin-stimulated rats. Data are expressed as mean ± SEM. Statistical analysis was performed with paired Student t-test.

	Control	*AG1295*	*P value*
Ovarian weight (mg) n = 12	20.85 ± 1.84	15.60 ± 1.14	$p < 0.05$
Estradiol (ng/ovary g) n = 6	146.8 ± 18.6	82.3 ± 16.1	$p < 0.05$
Progesterone (ng/ovary g) n = 6	946.2 ± 203.6	782.6 ± 163.0	NS

3.2. Ovarian weight and steroid hormone concentration

The effects of in vivo PDGFR inhibition on ovarian weight and steroid hormone concentrations are summarized in Table 2. The weight of AG1295-treated ovaries was significantly lower than that of control ovaries ($p < 0.01$, n = 12) (Table 2).

E_2 concentration in AG1295-treated ovaries decreased compared to untreated ovaries ($p < 0.05$), while P_4 concentration did not change in response to PDGFR inhibition (Table 2).

3.3. Follicular cell proliferation

Treatment with AG1295 decreased the proliferation index (PCNA-positive cells expressed as a percentage of the total number of cells) in comparison with untreated ovaries in both the granulosa cell compartment ($p < 0.01$) and the theca cell compartment ($p < 0.05$) (Fig. 2).

3.4. Ovarian apoptosis

EAFs from AG1295-treated ovaries showed a higher percentage of nuclei positive for cleaved caspase-3 than control follicles (Fig. 3A and B). This effect was observed in both follicular compartments (granulosa cells: $p < 0.05$; theca cells: $p < 0.01$).

Cultured EAFs from control and AG1295-treated ovaries exhibited typical DNA fragmentation in an internucleosomal pattern (Fig. 3C, lanes 2 and 3), while DNA fragmentation was minimal (no visible LMW DNA bands) in freshly isolated EAFs (Fig. 3C, lane 4). Quantification of LMW DNA fragments from EAFs revealed an increase (76%) in apoptotic DNA cleavage in AG1295-treated ovaries compared to controls (Fig. 3D; $p < 0.05$).

3.5. Proapoptotic and antiapoptotic protein expression

Expression of proapoptotic FAS, FASL, cleaved caspase-8, Bax and Bcl-X_S and antiapoptotic Bcl-2 and Bcl-X_L is presented in Figs. 4A

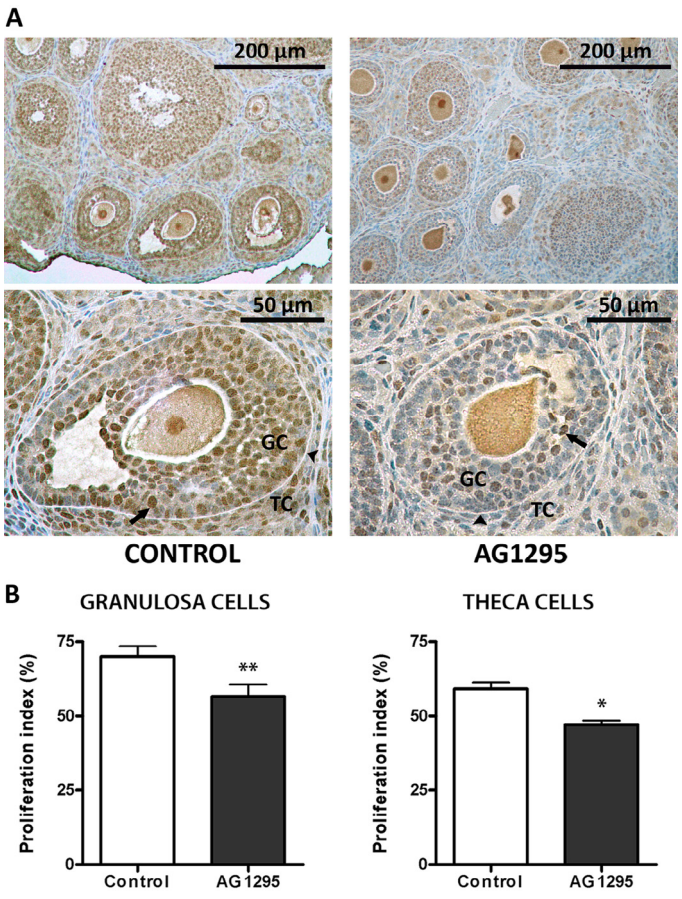

Fig. 2. Effect of AG1295 on the proliferation index of follicular cells. A: Micrographs of ovarian sections from control (left) and AG1295-treated (right) ovaries immunostained for PCNA. Top panels show representative ovarian areas at lower magnification whereas lower panels show representative EAFs at higher magnification. Arrows indicate immunopositive cells and arrowheads point towards the basal membrane. GC, granulosa cells; TC, theca cells. B: PCNA expression quantitation in granulosa and theca cells (n = 6). Data are expressed as mean ± SEM. $^{*}p < 0.05$; $^{**}p < 0.01$, paired Student t-test.

and 5. AG1295 increased the expression of Bax (Fig. 4B, $p < 0.05$) but did not change the expression of Bcl-2 (Fig. 4C) compared to untreated ovaries. AG1295 decreased both Bcl-2:Bax and Bcl-X_L:Bax ratios (Fig. 4D and F, $p < 0.05$). No changes were observed in the Bcl-X_L/Bcl-X_S ratio in comparison with control ovaries (Fig. 4E).

AG1295 did not significantly change FAS or FASL expression, (Fig. 5A and B), while AG1295-treated ovaries showed an increase in the cleavage of caspase-8, compared to control ovaries (Fig. 5C, $p < 0.05$).

3.6. Involvement of the PI3K/AKT pathway in cell survival

The expression of Ser 473-phosphorylated AKT (pAKT) and Ser 136-phosphorylated BAD (pBAD) in control and AG1295-treated ovaries is presented in Fig. 6. AG1295 decreased AKT phosphorylation (Fig. 6A; $p < 0.05$) and BAD phosphorylation compared with control ovaries (Fig. 6B, $p < 0.05$).

3.7. Evaluation of angiogenic parameters

Fig. 7A and 7B shows representative areas of ovarian sections stained with VWf or α-SMA. The RVA and mean cross-sectional area for VWf (endothelial cell marker) were decreased by AG1295 treatment (Fig. 7A and B, $p < 0.05$). Quantification of immunolabeling by α-SMA, a pericyte and VSMC marker, also showed a decrease in RVA and mean cross-sectional area of mature vessels in AG1295-treated ovaries in comparison with control ovaries (Fig. 7C and D, $p < 0.05$). No changes were observed regarding MVD between control and AG1295-treated ovaries in either VWf immunostaining (control: 1.104 ± 0.119; AG1295: 1.228 ± 0.137 vessels/10^6 pixels) or α-SMA immunostaining (control: 1.478 ± 0.310; AG1295: 1.137 ± 0.384 vessels/10^6 pixels).

4. Discussion

This study is the first to demonstrate that inhibition of the PDGF system by using a selective inhibitor of PDGFRs – locally injected under the bursa of the ovary – affects follicular development and steroid hormone concentrations, inhibits cell proliferation and induces apoptosis of follicular cells in eCG-treated rats. In addition, we showed that the intrabursal administration of a PDGFR inhibitor decreases blood vessel formation and stability in the ovaries from eCG-treated rats. These results suggest that the PDGF system is involved in the regulation of vascular development and in cell survival in the rat ovary.

The inhibition of PDGFR by AG1295 caused an increase in the percentage of AtrFs and a decrease in the percentage of PAFs and EAFs in gonadotropin-treated rat ovaries. These observations suggest that treatment with the PDGFR inhibitor alters follicular development, leading a greater number of follicles to atresia.

In this study, concentrations of P_4 in the ovarian tissue were unchanged among the different experimental groups, whereas ovarian E_2 concentrations were decreased by AG1295-treatment. This concurs with the results obtained by ovarian histology, which showed an alteration in follicular growth with a larger number of AtrFs after the treatment with the PDGFR inhibitor. These results suggest that the lower percentages of PAFs and EAFs caused by AG1295 treatment could be responsible for the low concentrations of ovarian estradiol, since follicular structures produce this steroid hormone.

We demonstrated that PDGFR inhibition by AG1295 resulted in a decrease in follicular cell proliferation in both the theca and granulosa compartments. These results are consistent with previous data observed by other investigators who showed an increase in theca cell proliferation after addition of PDGF ligands in rat and porcine theca-interstitial cells (Duleba et al., 1999; May et al., 1992). As cells undergo apoptosis during follicular degeneration by atresia, we evaluated the effect of PDGFR inhibition on the apoptotic process. The administration of AG1295 caused an increase in the percentage of apoptotic granulosa and theca cells, as well as in apoptotic DNA fragmentation in EAFs. These results indicate that PDGF would be a key limiting factor for follicular development and atresia.

Although many molecules, as Bcl-2 (Hsu and Hsueh, 2000; Tilly et al., 1995), Bcl-X (Parborell et al., 2002), Bax (Tilly et al., 1995) and caspases (Boone and Tsang, 1998; Flaws et al., 1995), have been implicated in the regulation of ovarian apoptosis, several studies have suggested that the activation of FAS by FASL plays a central role in the induction of follicular atresia (Kondo et al., 1996; Quirk et al., 1995). FAS is one of the death receptors belonging to the tumor necrosis factor (TNF) receptor superfamily. Death receptors are a subset of ligand-specific cell surface receptors that transmit apoptotic signals via a cytoplasmic death domain. Binding to their ligands induces recruitment and activation of caspases 8 and 10, which triggers a proteolytic cascade (Ashkenazi and Dixit, 1998; Guicciardi and Gores, 2009). Here, we showed that the protein expression of FAS and FASL remained unchanged after treatment with the inhibitor. Although the FAS/FASL system was not activated after treatment with AG1295, we observed that AG1295 increased the cleavage of caspase-8, chief initiator of the extrinsic mechanism of apoptosis. This suggests that the inhibition of PDGF may be activating other death receptors, such as TNF receptor 1 or TNF-α-related apoptosis-inducing ligand

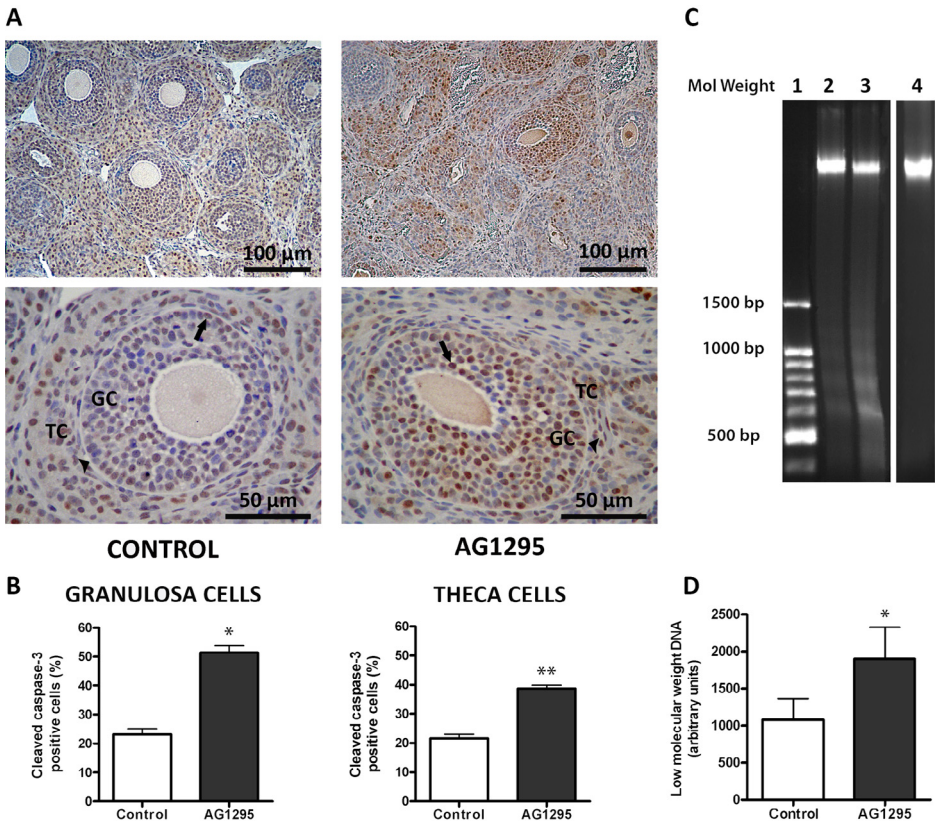

Fig. 3. Effect of AG1295 on ovarian apoptosis. A: Micrographs of ovarian sections immunostained for cleaved caspase-3 from a control ovary (left) and an AG1295-treated ovary (right). Top panels show representative ovarian areas at lower magnification whereas lower panels show representative EAFs at higher magnification. Arrows indicate immunopositive cells and arrowheads point towards the basal membrane. GC, granulosa cells; TC, theca cells. B: Cleaved caspase-3 quantitation in the granulosa and theca cell compartments (n = 6). C: Agarose gel electrophoresis of apoptotic DNA extracted from EAFs (representative lanes). Lane 1: DNA molecular weight marker; lane 2: control (24 h); lane 3: treated with the PDGFR inhibitor AG1295 (24 h); lane 4: negative control (0 h). D: Densitometric analysis of low molecular weight (LMW) DNA fragments (n = 6). Data are expressed as mean ± SEM. $^{*}p < 0.05$; $^{**}p < 0.01$, paired Student t-test.

receptor (TRAIL) (Hussein, 2005; Tartaglia et al., 1993; Wiley et al., 1995).

Numerous members of the *Bcl-2* gene family have been described as the main participants in the cascade of events that either activate or inhibit apoptosis (Boise et al., 1993). Bcl-2-related proteins can be separated into antiapoptotic and proapoptotic members, and the balance between these counteracting proteins presumably determines cell fate (Oltvai et al., 1993). In our experimental model, AG1295-treated ovaries showed increased expression of Bax without changes in Bcl-2, which causes a decrease not only in the Bcl-2/Bax ratio but also in the Bcl-X_L/Bax ratio and, in turn, causes apoptosis in follicular cells. Moreover, in AG1295-treated ovaries, no change was observed in the Bcl-X_L/Bcl-X_S ratio. Additionally, caspase-8 cleaves BID, a type *BH3-only* proapoptotic protein, which is able to activate Bax through a conformational change (Billen et al., 2008). Therefore, PDGFR inhibition could activate the intrinsic pathway (Bcl-2 family) as well as the extrinsic pathway (death receptors) of apoptosis during follicular development. Based on the data described earlier, PDGF would be acting as an intraovarian survival factor by suppressing apoptosis of follicular cells and thus rescuing follicles from atresia.

Although the most studied effects of PDGFs are those exerted on endothelial cells and pericytes (Arimura et al., 2012), in the last years there has been a growing body of evidence regarding the survival role of PDGFs in nonvascular cells, such as human macrophages and neurons (Peng et al., 2008; Son et al., 2014). Indeed, several studies have described PDGF as an antiapoptotic factor in tissues such as rat adrenal medulla and human prostate cancer cells (Iqbal et al., 2012; Yao and Cooper, 1995). Besides, Sleer and Taylor (2007a) described the presence of mRNA for all PDGF isoforms and receptors from neonatal period to adulthood, as well as the cellular localization of all members in oocytes and theca cells and of PDGFA and PDGFR-α in granulosa cells in the rat ovary (Sleer and Taylor, 2007a). The authors also suggested that these growth factors are implicated in preantral follicle growth. We have previously shown that other angiogenic factors, such as VEGF and ANGPTs, also act in rats as survival factors for ovarian follicular cells (Abramovich et al., 2006; Irusta et al., 2010; Parborell et al., 2011). Therefore, the mechanism of survival action of PDGF may be through an increase in vascular development or by a direct effect on receptors on follicular cells.

Several studies describe the signal transduction pathways of PDGF when it binds to its receptors, inducing a variety of cellular responses such as proliferation, survival and chemotaxis (Heldin and Westermark, 1999; Huang et al., 1984; Rocha et al., 2007; Yu et al., 2001). Our study showed that PDGFR inhibition caused a decrease in AKT phosphorylation at Ser 473. These results are consistent with data reported by other authors, such as Taylor et al. (2000), who demonstrated that treatment with PDGF in porcine theca cells increases phosphorylation of PDGFRβ and AKT/PKB at Ser 473, thus stimulating cell proliferation (Taylor, 2000). However, we cannot rule out the contribution of other signaling pathways such as Ras-Raf-MEK-ERK (Ras-Raf-MEK-ERK) to the effects of PDGF in the rat ovary. Regarding this point, Taylor et al. (2000) demonstrated that PDGF acts on porcine ovarian theca cells increasing cell proliferation, via activation of a Ras-mitogen-activated protein kinase-dependent

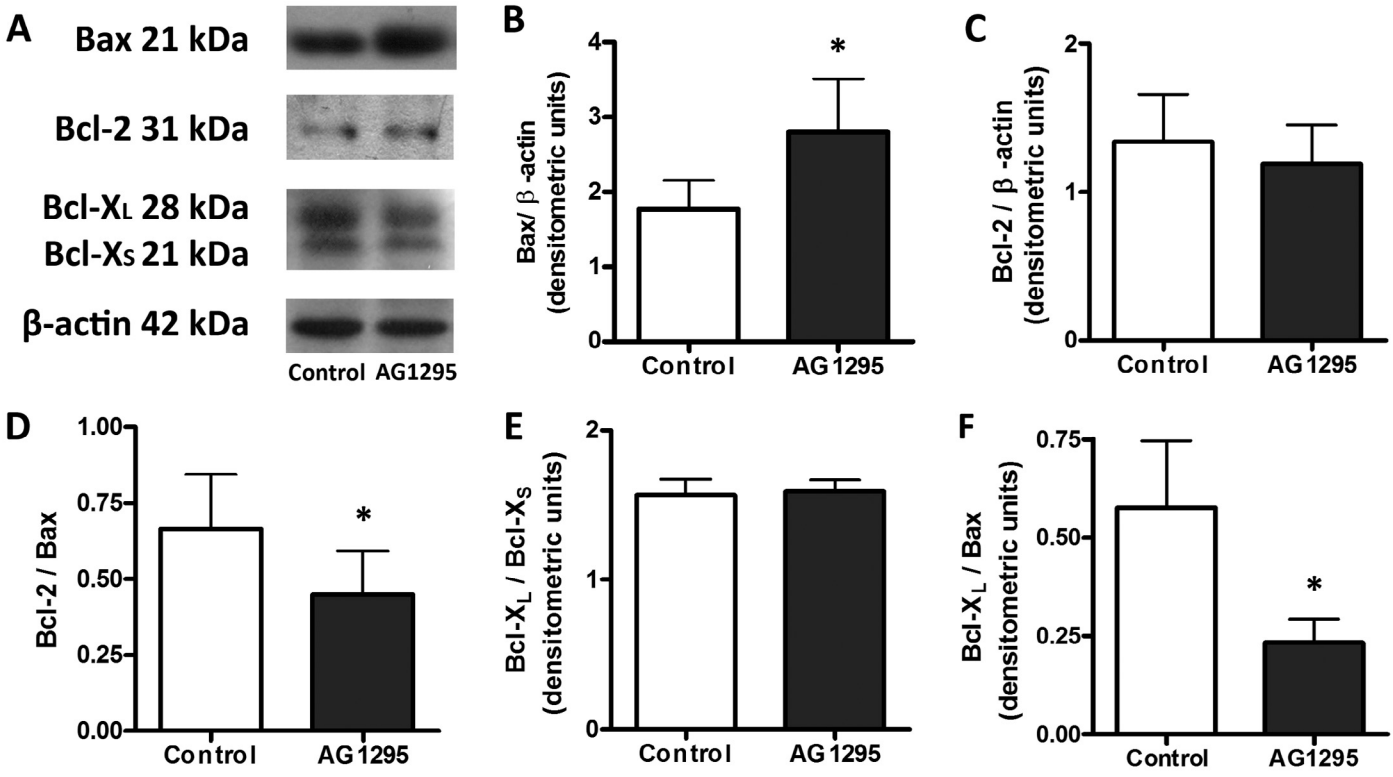

Fig. 4. Effect of AG1295 on pro- and antiapoptotic protein expression in rat ovarian tissue. A: A series of Western blot analyses from control and PDGFR-inhibited ovaries (AG1295) showing expression of Bax, Bcl-2, Bcl-$X_{L/S}$ and β-actin, as indicated. Adjacent bar graphs show the respective the densitometric quantification for each protein or protein ratio in control and AG1295-treated rat ovaries (n = 6). B: Densitometric analysis of Bax expression. C: Densitometric analysis of Bcl-2 expression. D: Densitometric analysis of Bcl-2/Bax ratio of expression. E: Densitometric analysis of Bcl-X_L/Bcl-X_S ratio of expression. F: Densitometric analysis of Bcl-X_L/Bax ratio of expression. In all cases, data are expressed as the mean ± SEM of three independent experiments and a representative blot of each protein is shown. *$p < 0.05$; paired Student t-test.

PI3-kinase-independent pathway (Taylor, 2000). Based on these data, we propose that the PI3K/AKT pathway is involved, at least partly, in the effects of PDGF on cell proliferation when bound to its receptor in the ovary.

One of the mechanisms by which AKT promotes cell survival is the inhibition of a proapoptotic member of the Bcl-2 family, BAD. This protein binds to the prosurvival protein Bcl-X_L and inhibits its function. Inactivation of BAD can be due to phosphorylation at two highly conserved sites, Ser 112 and Ser 136. When BAD is phosphorylated at either site, it dissociates from Bcl-X_L and binds to 14-3-3 proteins. Although Ser 112 corresponds to a consensus site for phosphorylation by AKT, AKT preferentially phosphorylates BAD at Ser 136 (Datta et al., 1999). In this study, we demonstrated that inhibition of PDGFR action in the ovary leads to a decrease in the phosphorylation of BAD at Ser 136. Taken together, our results suggest that inhibition of PDGFR leads to a decrease in AKT phosphorylation and consequently reduces BAD inactivation. Nonphosphorylated BAD would heterodimerize with BCL-X_L or Bcl-2

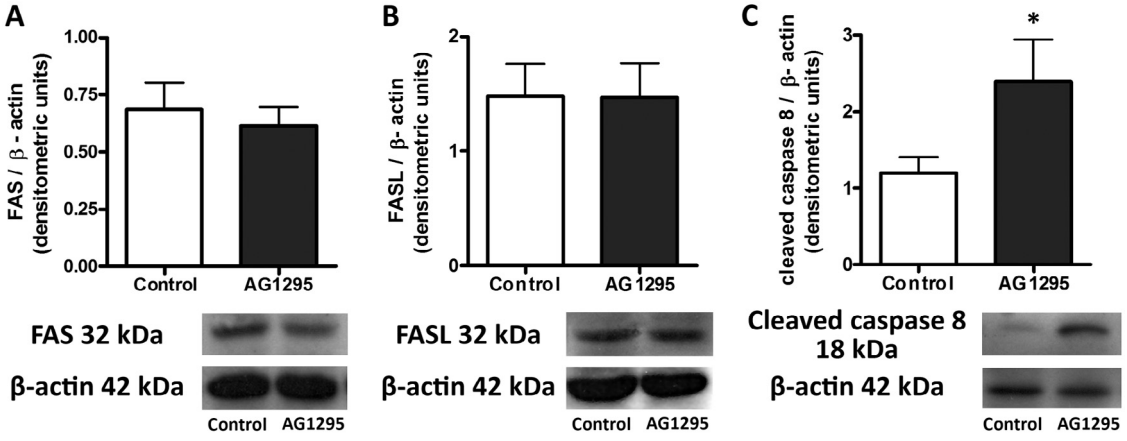

Fig. 5. Effect of AG1295 on the expression of proteins involved in the extrinsic apoptotic pathway. Protein expression of FAS, FASL and cleaved caspase-8. Upper panels show the densitometric quantification for each protein in control and AG1295-treated rat ovaries (n = 6). Lower panels show a representative blot for each protein analyzed. A: Densitometric analysis of FAS expression. B: Densitometric analysis of FASL expression. C: Densitometric analysis of cleaved caspase-8 expression. In all cases, data are expressed as the mean ± SEM of three independent experiments and a representative blot of each protein is shown. *$p < 0.05$; **$p < 0.01$; paired Student t-test.

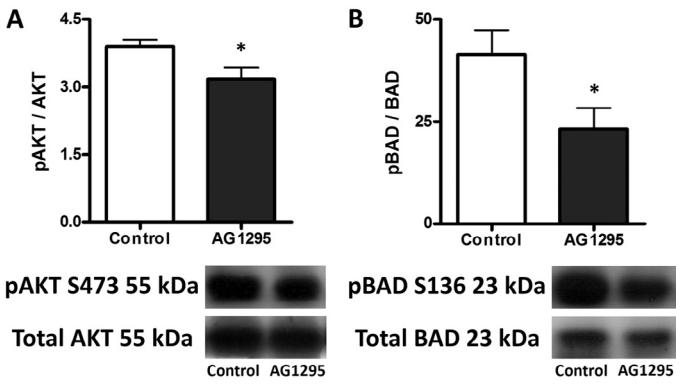

Fig. 6. Effect of AG1295 on the PI3K/AKT pathway in the rat ovary. Protein expression of phospho-AKT (pAKT), AKT, phospho-BAD (pBAD), BAD and β-actin (loading control), as indicated. Upper panels show the respective ratio of expression in control and AG1295-treated rat ovaries, obtained from densitometric quantification of these blots (n = 6). Lower panels show a representative blot for each protein analyzed. A: Densitometric analysis of the pAKT/AKT ratio of expression. B: Densitometric analysis of the pBAD/BAD ratio of expression. In all cases, data are expressed as the mean ± SEM of three independent experiments and a representative blot of each protein is shown. *$p < 0.05$; **$p < 0.01$; paired Student t-test.

proteins, thereby allowing the pro-apoptotic protein Bax to aggregate and induce release of cytochrome c, followed by caspase activation. Accordingly, the decrease in BAD phosphorylation may increase follicular cell apoptosis and follicular atresia. These results suggest that the PI3K/AKT pathway is involved in both the survival processes and the increase in proliferation rate induced by PDGF.

The formation of capillary networks in the ovary allows hormone-producing cells to obtain oxygen, nutrients and precursors to synthesize hormones for the regulation of the ovarian functions (Robinson et al., 2009; Tamanini and De Ambrogi, 2004). Follicular atresia is associated with inadequate development and/or regression of the thecal vasculature in most species studied (Barboni et al., 2000; Danforth et al., 2003; Girard et al., 2015; Hunter et al., 2004; Taylor et al., 2004; Wulff et al., 2001; Young and McNeilly, 2010). We found that the intrabursal administration of the PDGFR inhibitor caused a decrease not only in the endothelial cell area but also in the area of pericytes and VSMCs in the ovary, causing an alteration in vascular stability. This suggests that binding of PDGF ligands to their receptors would promote survival and proliferation in endothelial cells, as well as in pericytes and VSMCs.

Moreover, our study shows that the treatment with AG1295 caused erythrocyte extravasation into the antrum of follicles and

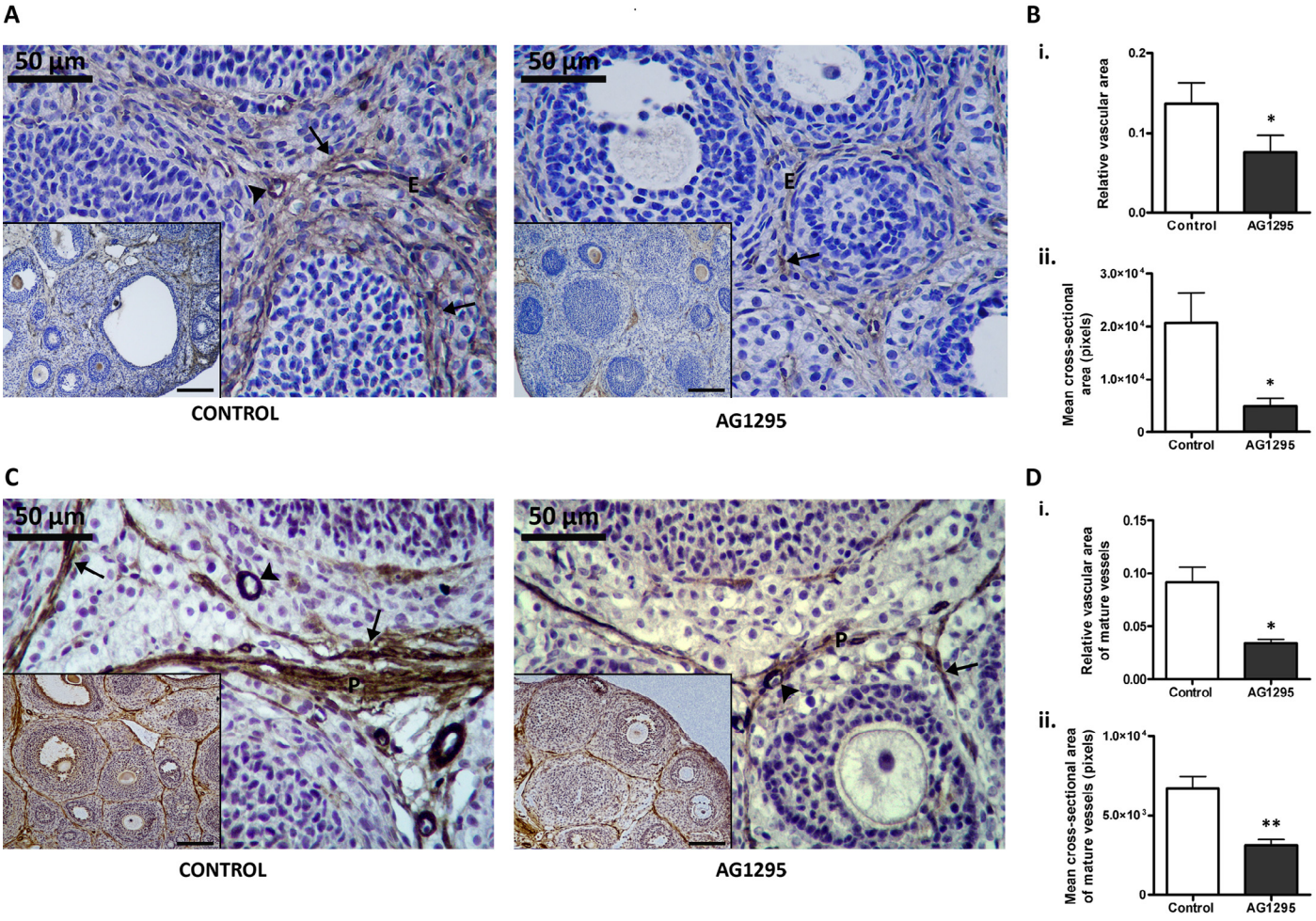

Fig. 7. Effect of AG1295 on ovarian vessels. A, C: Representative photographs of immunohistochemical staining for Von Willebrand factor (A) and α-SMA (C) in a control ovary (left panels) and an AG1295-treated ovary (right panels). Note the broad band of staining in the stromal and thecal compartments of the control ovary compared with the sparse staining in the AG1295-treated. Insets in all panels show lower magnification images showing a larger area of the ovary, with staining confined to vascular structures (arrows). Arrowheads indicate vessels in cross-section. Scale bars represent 50 µm (panels) and 150 µm (insets). E, endothelial cells; P, peri-endothelial cells (pericytes and VSMCs). B: Quantification of angiogenic parameters. (i) Relative vascular area (RVA); (ii) mean cross-sectional area of vessels. D: Quantification of angiogenic parameters. (i) Relative area occupied by mature vessels; (ii) mean cross-sectional area of mature vessels. Data are expressed as mean ± SEM. *$p < 0.05$; **$p < 0.01$, paired Student t-test.

widespread hemorrhagic destruction, suggesting an increased vascular permeability and vessel leakage. These results are consistent with the observations made by Leveen et al. (1994) and Soriano (1994), who have observed widespread microvascular leakage and hemorrhage in PDGFB and PDGFRβ knockout mice (Leveen et al., 1994; Soriano, 1994). Several studies have shown that PDGF plays a critical role in the recruitment of pericytes and VSMCs (Armulik et al., 2005). Studies performed by Leveen et al. (1994), Hellstrom et al. (2001) and Lindahl et al. (1997) have shown that PDGF-B deficient mice develop cardiovascular abnormalities, endothelial hyperplasia, capillary dilation and microaneurysms, thus emphasizing the importance of the PDGF system in vascular maturity and functionality (Hellstrom et al., 2001; Leveen et al., 1994; Lindahl et al., 1997). We propose that the mechanisms by which inhibition of PDGF exerts this regulatory action on follicular development could be through the regulation of vascular development, that in turn promotes proper follicular development and corpus luteum formation or through a direct effect on follicular cells. More studies are needed to elucidate this issue.

In summary, we showed that AG1295 diminished the percentage of PAFs and EAFs, as well as the ovarian weight, E_2 concentration and proliferation of follicular cells. PDGFR inhibition also increased the percentage of AtrFs, the percentage of positive nuclei for cleaved caspase-3 and apoptotic DNA fragmentation. Our results suggest that this increase in atresia is mediated by ovarian apoptosis through an imbalance in the ratio of antiapoptotic to proapoptotic proteins. Moreover, AG1295 decreased the endothelial cell area and the pericytes and VMSCs area, affecting vascular stability. PDGFs could be exerting their mechanism of action through an autocrine/paracrine effect on granulosa and theca cells mediated by PDGFRs. This indicates that PDGFs would act not only as angiogenic factors but also as survival factors during folliculogenesis in the rat ovary.

Our data indicate that the PDGF system is necessary for follicular development induced by gonadotropins. However, more information is required to elucidate the relevance of the changes observed in the vascular network during follicular development and to clarify the interactions between the PDGF system and the essential hormones for normal ovarian function.

Finally, the understanding of the physiology of angiogenic factors proves to be essential to propose prevention/prediction measures and to develop new therapeutic strategies for many female reproductive disorders.

Acknowledgements

This study was supported by ANPCyT (PICT 2008/747), CONICET (PIP 1223) and Roemmers Foundation, Argentina.

Appendix: Supplementary material

Supplementary data to this article can be found online at doi:10.1016/j.mce.2015.04.021.

References

Abramovich, D., Parborell, F., Tesone, M., 2006. Effect of a vascular endothelial growth factor (VEGF) inhibitory treatment on the folliculogenesis and ovarian apoptosis in gonadotropin-treated prepubertal rats. Biol. Reprod. 75, 434–441.

Andreu, C., Parborell, F., Vanzulli, S., Chemes, H., Tesone, M., 1998. Regulation of follicular luteinization by a gonadotropin-releasing hormone agonist: relationship between steroidogenesis and apoptosis. Mol. Reprod. Dev. 51, 287–294.

Arimura, K., Ago, T., Kamouchi, M., Nakamura, K., Ishitsuka, K., Kuroda, J., et al., 2012. PDGF receptor beta signaling in pericytes following ischemic brain injury. Curr. Neurovasc. Res. 9, 1–9.

Armulik, A., Abramsson, A., Betsholtz, C., 2005. Endothelial/pericyte interactions. Circ. Res. 97, 512–523.

Ashkenazi, A., Dixit, V.M., 1998. Death receptors: signaling and modulation. Science 281, 1305–1308.

Banai, S., Wolf, Y., Golomb, G., Pearle, A., Waltenberger, J., Fishbein, I., et al., 1998. PDGF-receptor tyrosine kinase blocker AG1295 selectively attenuates smooth muscle cell growth in vitro and reduces neointimal formation after balloon angioplasty in swine. Circulation 97, 1960–1969.

Barboni, B., Turriani, M., Galeati, G., Spinaci, M., Bacci, M.L., Forni, M., et al., 2000. Vascular endothelial growth factor production in growing pig antral follicles. Biol. Reprod. 63, 858–864.

Billen, L.P., Shamas-Din, A., Andrews, D.W., 2008. Bid: a Bax-like BH3 protein. Oncogene 27 (Suppl. 1), S93–S104.

Boise, L.H., Gonzalez-Garcia, M., Postema, C.E., Ding, L., Lindsten, T., Turka, L.A., et al., 1993. bcl-x, a bcl-2-related gene that functions as a dominant regulator of apoptotic cell death. Cell 74, 597–608.

Boone, D.L., Tsang, B.K., 1998. Caspase-3 in the rat ovary: localization and possible role in follicular atresia and luteal regression. Biol. Reprod. 58, 1533–1539.

Choi, J.Y., Jo, M.W., Lee, E.Y., Yoon, B.K., Choi, D.S., 2010. The role of autophagy in follicular development and atresia in rat granulosa cells. Fertil. Steril. 93, 2532–2537.

Chun, S.Y., Billig, H., Tilly, J.L., Furuta, I., Tsafriri, A., Hsueh, A.J., 1994. Gonadotropin suppression of apoptosis in cultured preovulatory follicles: mediatory role of endogenous insulin-like growth factor I. Endocrinology 135, 1845–1853.

Chun, S.Y., Eisenhauer, K.M., Minami, S., Billig, H., Perlas, E., Hsueh, A.J., 1996. Hormonal regulation of apoptosis in early antral follicles: follicle-stimulating hormone as a major survival factor. Endocrinology 137, 1447–1456.

Claesson-Welsh, L., 1996. Mechanism of action of platelet-derived growth factor. Int. J. Biochem. Cell Biol. 28, 373–385.

Danforth, D.R., Arbogast, L.K., Ghosh, S., Dickerman, A., Rofagha, R., Friedman, C.I., 2003. Vascular endothelial growth factor stimulates preantral follicle growth in the rat ovary. Biol. Reprod. 68, 1736–1741.

Datta, S.R., Brunet, A., Greenberg, M.E., 1999. Cellular survival: a play in three Akts. Genes Dev. 13, 2905–2927.

Dhanasekaran, N., Moudgal, N.R., 1989. Studies on follicular atresia: role of gonadotropins and gonadal steroids in regulating cathepsin-D activity of preovulatory follicles in the rat. Mol. Cell. Endocrinol. 63, 133–142.

Duleba, A.J., Spaczynski, R.Z., Arici, A., Carbone, R., Behrman, H.R., 1999. Proliferation and differentiation of rat theca-interstitial cells: comparison of effects induced by platelet-derived growth factor and insulin-like growth factor-I. Biol. Reprod. 60, 546–550.

Flaws, J.A., Kugu, K., Trbovich, A.M., DeSanti, A., Tilly, K.I., Hirshfield, A.N., et al., 1995. Interleukin-1 beta-converting enzyme-related proteases (IRPs) and mammalian cell death: dissociation of IRP-induced oligonucleosomal endonuclease activity from morphological apoptosis in granulosa cells of the ovarian follicle. Endocrinology 136, 5042–5053.

Fraser, H.M., Wulff, C., 2003. Angiogenesis in the corpus luteum. Reprod. Biol. Endocrinol. 1, 88.

Girard, A., Dufort, I., Douville, G., Sirard, M.A., 2015. Global gene expression in granulosa cells of growing, plateau and atretic dominant follicles in cattle. Reprod. Biol. Endocrinol. 13, 10.

Guicciardi, M.E., Gores, G.J., 2009. Life and death by death receptors. FASEB J. 23, 1625–1637.

Heldin, C.H., Westermark, B., 1999. Mechanism of action and in vivo role of platelet-derived growth factor. Physiol. Rev. 79, 1283–1316.

Heldin, C.H., Ostman, A., Ronnstrand, L., 1998. Signal transduction via platelet-derived growth factor receptors. Biochim. Biophys. Acta 1378, F79–F113.

Hellstrom, M., Kalen, M., Lindahl, P., Abramsson, A., Betsholtz, C., 1999. Role of PDGF-B and PDGFR-beta in recruitment of vascular smooth muscle cells and pericytes during embryonic blood vessel formation in the mouse. Development 126, 3047–3055.

Hellstrom, M., Gerhardt, H., Kalen, M., Li, X., Eriksson, U., Wolburg, H., et al., 2001. Lack of pericytes leads to endothelial hyperplasia and abnormal vascular morphogenesis. J. Cell Biol. 153, 543–553.

Hsu, S.Y., Hsueh, A.J., 2000. Tissue-specific Bcl-2 protein partners in apoptosis: An ovarian paradigm. Physiol. Rev. 80, 593–614.

Huang, J.S., Huang, S.S., Deuel, T.F., 1984. Transforming protein of simian sarcoma virus stimulates autocrine growth of SSV-transformed cells through PDGF cell-surface receptors. Cell 39, 79–87.

Hughes, F.M., Jr., Gorospe, W.C., 1991. Biochemical identification of apoptosis (programmed cell death) in granulosa cells: evidence for a potential mechanism underlying follicular atresia. Endocrinology 129, 2415–2422.

Hunter, M.G., Robinson, R.S., Mann, G.E., Webb, R., 2004. Endocrine and paracrine control of follicular development and ovulation rate in farm species. Anim. Reprod. Sci. 82–83, 461–477.

Hussein, M.R., 2005. Apoptosis in the ovary: molecular mechanisms. Hum. Reprod. Update 11, 162–177.

Hwu, Y.M., Li, S.H., Lee, R.K., Lin, M.H., Tsai, Y.H., Yeh, T.S., 2009. Luteinizing hormone increases platelet-derived growth factor-D gene expression in human granulosa-luteal cells. Fertil. Steril. 92, 2065–2068.

Iqbal, S., Zhang, S., Driss, A., Liu, Z.R., Kim, H.R., Wang, Y., et al., 2012. PDGF upregulates Mcl-1 through activation of beta-catenin and HIF-1alpha-dependent signaling in human prostate cancer cells. PLoS ONE 7, e30764.

Irusta, G., Parborell, F., Peluffo, M., Manna, P.R., Gonzalez-Calvar, S.I., Calandra, R., et al., 2003. Steroidogenic acute regulatory protein in ovarian follicles of gonadotropin-stimulated rats is regulated by a gonadotropin-releasing hormone agonist. Biol. Reprod. 68, 1577–1583.

Irusta, G., Parborell, F., Tesone, M., 2007. Inhibition of cytochrome P-450 C17 enzyme by a GnRH agonist in ovarian follicles from gonadotropin-stimulated rats. Am. J. Physiol. Endocrinol. Metab. 292, E1456–E1464.
Irusta, G., Abramovich, D., Parborell, F., Tesone, M., 2010. Direct survival role of vascular endothelial growth factor (VEGF) on rat ovarian follicular cells. Mol. Cell. Endocrinol. 325, 93–100.
Kaczmarek, M.M., Schams, D., Ziecik, A.J., 2005. Role of vascular endothelial growth factor in ovarian physiology – an overview. Reprod. Biol. 5, 111–136.
Kondo, H., Maruo, T., Peng, X., Mochizuki, M., 1996. Immunological evidence for the expression of the Fas antigen in the infant and adult human ovary during follicular regression and atresia. J. Clin. Endocrinol. Metab. 81, 2702–2710.
Kuhnert, F., Tam, B.Y., Sennino, B., Gray, J.T., Yuan, J., Jocson, A., et al., 2008. Soluble receptor-mediated selective inhibition of VEGFR and PDGFRbeta signaling during physiologic and tumor angiogenesis. Proc. Natl. Acad. Sci. U.S.A. 105, 10185–10190.
LaRochelle, W.J., Jeffers, M., McDonald, W.F., Chillakuru, R.A., Giese, N.A., Lokker, N.A., et al., 2001. PDGF-D, a new protease-activated growth factor. Nat. Cell Biol. 3, 517–521.
Leveen, P., Pekny, M., Gebre-Medhin, S., Swolin, B., Larsson, E., Betsholtz, C., 1994. Mice deficient for PDGF B show renal, cardiovascular, and hematological abnormalities. Genes Dev. 8, 1875–1887.
Levitzki, A., Gazit, A., 1995. Tyrosine kinase inhibition: an approach to drug development. Science 267, 1782–1788.
Li, X., Ponten, A., Aase, K., Karlsson, L., Abramsson, A., Uutela, M., et al., 2000. PDGF-C is a new protease-activated ligand for the PDGF alpha-receptor. Nat. Cell Biol. 2, 302–309.
Lindahl, P., Johansson, B.R., Leveen, P., Betsholtz, C., 1997. Pericyte loss and microaneurysm formation in PDGF-B-deficient mice. Science 277, 242–245.
May, J.V., Bridge, A.J., Gotcher, E.D., Gangrade, B.K., 1992. The regulation of porcine theca cell proliferation in vitro: synergistic actions of epidermal growth factor and platelet-derived growth factor. Endocrinology 131, 689–697.
McGee, E.A., Chun, S.Y., Lai, S., He, Y., Hsueh, A.J., 1999. Keratinocyte growth factor promotes the survival, growth, and differentiation of preantral ovarian follicles. Fertil. Steril. 71, 732–738.
McNatty, K.P., Heath, D.A., Lundy, T., Fidler, A.E., Quirke, L., O'Connell, A., et al., 1999. Control of early ovarian follicular development. J. Reprod. Fertil. Suppl. 54, 3–16.
Nilsson, E.E., Detzel, C., Skinner, M.K., 2006. Platelet-derived growth factor modulates the primordial to primary follicle transition. Reproduction 131, 1007–1015.
Oltvai, Z.N., Milliman, C.L., Korsmeyer, S.J., 1993. Bcl-2 heterodimerizes in vivo with a conserved homolog, Bax, that accelerates programmed cell death. Cell 74, 609–619.
Parborell, F., Dain, L., Tesone, M., 2001. Gonadotropin-releasing hormone agonist affects rat ovarian follicle development by interfering with FSH and growth factors on the prevention of apoptosis. Mol. Reprod. Dev. 60, 241–247.
Parborell, F., Pecci, A., Gonzalez, O., Vitale, A., Tesone, M., 2002. Effects of a gonadotropin-releasing hormone agonist on rat ovarian follicle apoptosis: Regulation by EGF and the expression of Bcl-2-related genes. Biol. Reprod. 67, 481–486.
Parborell, F., Irusta, G., Vitale, A.M., Gonzalez, O., Pecci, A., Tesone, M., 2005. GnRH antagonist Antide inhibits apoptosis of preovulatory follicle cells in rat ovary. Biol. Reprod. 72, 659–666.
Parborell, F., Abramovich, D., Tesone, M., 2008. Intrabursal administration of the antiangiopoietin 1 antibody produces a delay in rat follicular development associated with an increase in ovarian apoptosis mediated by changes in the expression of BCL2 related genes. Biol. Reprod. 78, 506–513.
Parborell, F., Abramovich, D., Irusta, G., Tesone, M., 2011. Angiopoietin 1 reduces rat follicular atresia mediated by apoptosis through the PI3K/Akt pathway. Mol. Cell. Endocrinol. 343, 79–87.
Peng, F., Dhillon, N., Callen, S., Yao, H., Bokhari, S., Zhu, X., et al., 2008. Platelet-derived growth factor protects neurons against gp120-mediated toxicity. J. Neurovirol. 14, 62–72.
Pinkas, H., Fisch, B., Rozansky, G., Felz, C., Kessler-Icekson, G., Krissi, H., et al., 2008. Platelet-derived growth factors (PDGF-A and -B) and their receptors in human fetal and adult ovaries. Mol. Hum. Reprod. 14, 199–206.
Quirk, S.M., Cowan, R.G., Joshi, S.G., Henrikson, K.P., 1995. Fas antigen-mediated apoptosis in human granulosa/luteal cells. Biol. Reprod. 52, 279–287.
Redmer, D.A., Reynolds, L.P., 1996. Angiogenesis in the ovary. Rev. Reprod. 1, 182–192.
Redmer, D.A., Doraiswamy, V., Bortnem, B.J., Fisher, K., Jablonka-Shariff, A., Grazul-Bilska, A.T., et al., 2001. Evidence for a role of capillary pericytes in vascular growth of the developing ovine corpus luteum. Biol. Reprod. 65, 879–889.
Robinson, R.S., Woad, K.J., Hammond, A.J., Laird, M., Hunter, M.G., Mann, G.E., 2009. Angiogenesis and vascular function in the ovary. Reproduction 138, 869–881.
Rocha, A., Azevedo, I., Soares, R., 2007. Anti-angiogenic effects of imatinib target smooth muscle cells but not endothelial cells. Angiogenesis 10, 279–286.
Sadrkhanloo, R., Hofeditz, C., Erickson, G.F., 1987. Evidence for widespread atresia in the hypophysectomized estrogen-treated rat. Endocrinology 120, 146–155.
Sleer, L.S., Taylor, C.C., 2007a. Cell-type localization of platelet-derived growth factors and receptors in the postnatal rat ovary and follicle. Biol. Reprod. 76, 379–390.
Sleer, L.S., Taylor, C.C., 2007b. Platelet-derived growth factors and receptors in the rat corpus luteum: localization and identification of an effect on luteogenesis. Biol. Reprod. 76, 391–400.
Son, D., Na, Y.R., Hwang, E.S., Seok, S.H., 2014. Platelet-derived growth factor-C (PDGF-C) induces anti-apoptotic effects on macrophages through Akt and Bad phosphorylation. J. Biol. Chem. 289, 6225–6235.
Soriano, P., 1994. Abnormal kidney development and hematological disorders in PDGF beta-receptor mutant mice. Genes Dev. 8, 1888–1896.
Suzuki, T., Sasano, H., Takaya, R., Fukaya, T., Yajima, A., Nagura, H., 1998. Cyclic changes of vasculature and vascular phenotypes in normal human ovaries. Hum. Reprod. 13, 953–959.
Tamanini, C., De Ambrogi, M., 2004. Angiogenesis in developing follicle and corpus luteum. Reprod. Domest. Anim. 39, 206–216.
Tartaglia, L.A., Ayres, T.M., Wong, G.H., Goeddel, D.V., 1993. A novel domain within the 55 kd TNF receptor signals cell death. Cell 74, 845–853.
Taylor, C.C., 2000. Platelet-derived growth factor activates porcine thecal cell phosphatidylinositol-3-kinase-Akt/PKB and ras-extracellular signal-regulated kinase-1/2 kinase signaling pathways via the platelet-derived growth factor-beta receptor. Endocrinology 141, 1545–1553.
Taylor, P.D., Hillier, S.G., Fraser, H.M., 2004. Effects of GnRH antagonist treatment on follicular development and angiogenesis in the primate ovary. J. Endocrinol. 183, 1–17.
Tilly, J.L., Billig, H., Kowalski, K.I., Hsueh, A.J., 1992. Epidermal growth factor and basic fibroblast growth factor suppress the spontaneous onset of apoptosis in cultured rat ovarian granulosa cells and follicles by a tyrosine kinase-dependent mechanism. Mol. Endocrinol. 6, 1942–1950.
Tilly, J.L., Tilly, K.I., Kenton, M.L., Johnson, A.L., 1995. Expression of members of the bcl-2 gene family in the immature rat ovary: equine chorionic gonadotropin-mediated inhibition of granulosa cell apoptosis is associated with decreased bax and constitutive bcl-2 and bcl-x long messenger ribonucleic acid levels. Endocrinology 136, 232–241.
Uren, A., Yu, J.C., Gholami, N.S., Pierce, J.H., Heidaran, M.A., 1994. The alpha PDGFR tyrosine kinase mediates locomotion of two different cell types through chemotaxis and chemokinesis. Biochem. Biophys. Res. Commun. 204, 628–634.
Wiley, S.R., Schooley, K., Smolak, P.J., Din, W.S., Huang, C.P., Nicholl, J.K., et al., 1995. Identification and characterization of a new member of the TNF family that induces apoptosis. Immunity 3, 673–682.
Woodruff, T.K., D'Agostino, J., Schwartz, N.B., Mayo, K.E., 1988. Dynamic changes in inhibin messenger RNAs in rat ovarian follicles during the reproductive cycle. Science 239, 1296–1299.
Wulff, C., Wiegand, S.J., Saunders, P.T., Scobie, G.A., Fraser, H.M., 2001. Angiogenesis during follicular development in the primate and its inhibition by treatment with truncated Flt-1-Fc (vascular endothelial growth factor Trap(A40). Endocrinology 142, 3244–3254.
Yao, R., Cooper, G.M., 1995. Requirement for phosphatidylinositol-3 kinase in the prevention of apoptosis by nerve growth factor. Science 267, 2003–2006.
Yoon, S.J., Kim, K.H., Chung, H.M., Choi, D.H., Lee, W.S., Cha, K.Y., et al., 2006. Gene expression profiling of early follicular development in primordial, primary, and secondary follicles. Fertil. Steril. 85, 193–203.
Young, J.M., McNeilly, A.S., 2010. Theca: the forgotten cell of the ovarian follicle. Reproduction 140, 489–504.
Yu, J., Moon, A., Kim, H.R., 2001. Both platelet-derived growth factor receptor (PDGFR)-alpha and PDGFR-beta promote murine fibroblast cell migration. Biochem. Biophys. Res. Commun. 282, 697–700.
Zhang, Y.Y., Cui, Y.Z., Luan, J., Zhou, X.Y., Zhang, G.L., Han, J.X., 2012. Platelet-derived growth factor receptor kinase inhibitor AG-1295 promotes osteoblast differentiation in MC3T3-E1 cells via the Erk pathway. Biosci. Trends 6, 130–135.